Neuro-Oncology

Neuro-Oncology 16(1), 72–80, 2014
doi:10.1093/neuonc/not152
Advance Access date 16 December 2013

Development of transplantable human chordoma xenograft for preclinical assessment of novel therapeutic strategies

Fabio Bozzi, Giacomo Manenti, Elena Conca, Silvia Stacchiotti, Antonella Messina, GianPaolo Dagrada, Alessandro Gronchi, Pietro Panizza, Marco A. Pierotti, Elena Tamborini, and Silvana Pilotti

Department of Pathology, Laboratory of Experimental Molecular Pathology (F.B., E.C., G.D., E.T., S.P.); Department of Experimental Oncology (G.M.); Department of Cancer Medicine, Sarcoma Unit (S.S.); Department of Radiology (A.M., P.P.); Department of Surgery (A.G.); Scientific Director (M.A.P.), Fondazione IRCCS Istituto Nazionale dei Tumori, Milan, Italy

Corresponding author: Elena Tamborini, Experimental Molecular Pathology, Department of Pathology, Fondazione IRCCS Istituto Tumori Milano, Via G. Venezian 1, 20133 Milano, Italy. (elena.tamborini@istitutotumori.mi.it).

Background. Chordomas are rare and indolent bone tumors that arise in the skull base and mobile spine. Distant metastases occur in >20% of cases, but morbidity and mortality are mainly related to local relapses that affect the majority of patients. Standard chemotherapy has modest activity, whereas new targeted therapies (alone or in combination) have some activity in controlling disease progression. However, the scarcity of preclinical models capable of testing in vivo responses to these therapies hampers the development of new medical strategies.

Methods. In this study, 8 chordoma samples taken from 8 patients were implanted in nude mice. Four engrafted successfully and gave rise to tumor masses that were analyzed histologically, by means of fluorescence *in situ* hybridization and biochemical techniques. The data relating to each of the mouse tumors were compared with those obtained from the corresponding human tumor.

Results. All 4 engraftments retained the histological, genetic and biochemical features of the human tumors they came from. In one epidermal growth factor receptor(EGFR)-positive xenograft, responsiveness to lapatinib was evaluated by comparing the pre- and post-treatment findings. The treatment induced a low-level, heterogeneous switching off of EGFR and its downstream signaling effectors.

Conclusions. Overall, this model is very close to human chordoma and represents a new means of undertaking preclinical investigations and developing tailored therapies.

Keywords: chordoma, EGFR, preclinical model, tailored therapies.

Chordomas are rare bone tumors (estimated incidence ~0.1/100 000) that originate from remnants of the notochord and molecularly express the transcription factor brachyury. They mainly affect the sacrum (50%–60%) and skull base (25%–35%) and less frequently arise from the vertebral axis (5%).[1] The location of the primary disease makes treatment highly challenging. Surgery (the standard treatment) is frequently not curative because of the incomplete removal of the tumor, which affects the long-term prognosis of most chordoma patients. Cytotoxic chemotherapy has modest activity,[2] and therefore high-dose radiation therapy is used for inoperable cases.

Over the last 10 years, a number of chordoma molecular targets have been identified[3–6] but the inhibitors used so far[7–9] have been chosen on the basis of the expression/activation profiles of their targets in cryopreserved surgical samples without any preclinical evaluation of their activity in terms of tumor stabilization/shrinkage, antivasculature effects, paracrine-signaling inhibition, or metastases. It is therefore clear that chordoma models are needed for preclinical tests.

Although an increasing number of chordoma cell lines have been established as a result of the contribution of the Chordoma Foundation (www.chordoma.org), they are not always available and do not mirror the tumor microenvironment.

In the search for suitable preclinical models, we concentrated on grafting human chordoma samples into immune-deficient mice[10,11] because this perpetuation retains and recapitulates the characteristics of the original tumor and may predict the response to target treatment better than immortalized cell lines. The need for a chordoma model has been indirectly strengthened by recent findings demonstrating that: (i) brachyury (the chordoma master gene) indirectly regulates the expression of selected integrins, adhesion molecules, and growth factors;[12,13] and (ii) the extracellular

Received 25 January 2013; accepted 21 August 2013

matrix, whose chordoma is particularly rich,[14] may act as a cofactor in the development of resistance to targeted therapies.[15]

We describe the characterization of 4 human chordoma xenografts that adequately recapitulate the biological features of human chordomas. One epidermal growth factor receptor (EGFR)-positive chordoma grew as a continuous xenograft: this was used as a proof. On the basis of the findings of an ongoing clinical trial at the time,[9] the mouse was treated with lapatinib, which showed some activity in terms of radiological and pathological responses and target switch-off.

Material and Methods

Patients

Between 2007 and 2010, tumor tissues suitable for mouse implantation were obtained from 8 surgically treated patients with sacral chordoma (6 primary tumors and 2 recurrences). The morphological diagnosis of chordoma was based on the criteria proposed in the WHO classification[16] and was confirmed by brachyury nuclear immunoreactivity.

Two of the patients had been previously treated with chemotherapy and/or targeted therapy (imatinib or imatinib + sirolimus), but the time between the last pharmacological treatment and surgery was more than 3 months (Table 1). The samples for implantation were obtained directly from the operating theater under sterile conditions. This study was approved by the institutional review board (Independent Ethics Committee) of Fondazione IRCCS Istituto Nazionale dei Tumori – Milan, and all patients gave their written informed consent.

Human Samples

As described in the supplementary material (on line at http://neuro-oncology.oxfordjournals.org), the samples were assessed by means of an receptor tyrosine kinase (RTK) expression assay, a fluorescence *in situ* hybridization (FISH) analysis, an RTK activation assay, and a downstream signaling analysis.

Animals

Female athymic CD-1 *nu/nu* mice were kept under specific pathogen-free conditions in the animal research facilities of our Department of Experimental Oncology and Molecular Medicine (Fondazione IRCCS Istituto Nazionale dei Tumori, Milan, Italy). The procedures involving the animals and their care were carried out in accordance with the regulations of our Ethics Committee for Animal Experimentation, and Italian and European laws and policies.

Human Chordoma Implantation

Before any implantation, the representativeness of the fresh human tumor samples was checked in hematoxylin and eosin(H&E)-stained frozen sections. The tumor xenografts were established by subcutaneously injecting human tumor fragments of about 4×4 mm into the flanks of 5- or 6-week-old female CD-1 *nu/nu* mice under general anesthesia. Two to 4 animals were used for each specimen depending on tissue availability. The growth of the tumors was followed by measuring their diameters every week using Vernier calipers. At the end of the observation period, the mice were anesthetized with isoflurane and killed by means of cervical dislocation. A xenograft model was considered established after 2 serial passages. The obtained xenografts were partly used for further transplantation and partly snap frozen. The frozen material was stained with H&E and underwent FISH and biochemical analyses, including brachyury and downstream signaling, and the results were compared with the corresponding human sample.

Comparison of Human Samples and Corresponding Mouse Xenografts

Brachyury expression in fixed mouse material was evaluated by means of an immunofluorescence assay using the antibrachyury antibody (SC-20109, Santa Cruz) diluted 1:200. The antigen was retrieved using 1 mmol/EDTA, pH 8, in an autoclave at 95°C for 15 minutes. The assay was carried out using an Alexa 546 anti-rabbit secondary antibody diluted 1:1000 at room temperature for 60 minutes. The chordoma cells were counterstained with conjugated anti-CAM 5.2 FITC (Becton Dickinson) and DAPI.

Table 1. Chordoma samples and their clinical, pathological and biochemical characterization.

Human chordoma characteristics and medical treatments				IHC analysis of formalin-fixed paraffin-embedded material			Biochemical analysis of frozen material before mouse implantation			
Patient No.	Site	Primary/ recurrence	Medical treatment	Brach	PDGFRB	EGFR	Brach	pPDGFRB pRTK assay results	pPDGFRB IP/WB results	pEGFR pRTK assay results
1	S	P	Imatinib and imatinib plus sirolimus	+	+	+	+	−/+	−/+	+
2	S	R	Untreated	+	+	+	+	+	+	+
3	S	R	Imatinib	+	+	+	+	−	+	+
4	S	P	Untreated	+	+	+	+	−	+	+
5	S	P	Untreated	+	+	+	+	+	+	+
6	S	P	Untreated	+	NE	NE	+	+	+	+
7	S	P	Untreated	+	NE	NE	+	−	NA	+
8	S	P	Untreated	+	−	+	+	−	NA	+

RTK expression/activation was evaluated by means of immunohistochemistry (IHC) phospo RTK array (pRTK assay) and immunoprecipitation/Western blot (IP/WB). All of the cases showed EGFR activation (pRTK array). This study was approved by the institutional review board (Independent Ethics Committee) of Fondazione IRCCS Istituto Nazionale dei Tumori – Milan, and all patients gave their written informed consent.

Abbreviations: Brach, brachyury; IHC, immunohistochemistry; NA, not analyzed; NE, not evaluable; P, primary; R, recurrence; S, sacrum; −, negative; +, positive

Brachyury expression in frozen human and mouse material was assessed by means of a Western blotting(WB)-based analysis using the antibrachyury antibody (Santa Cruz) diluted 1:1000, and RTK downstream signaling analyses were made using previously described protocols.[5]

The FISH probe set included EGFR/CEP7, HER2/CEP17 and p16/CEP9 (Vysis), and the analyses were made using previously described protocols.[5]

Xenograft Lapatinib Treatment

Three mouse samples obtained during the third passage (P3) of xenografts derived from patient 5 (Table 1) were treated with lapatinib. The drug (cat: S1028, Selleck Chemical) was resuspended in 80% methylcellulose, 10% Tween 80%, and 10% DMSO[17].

Evaluation of Lapatinib Effects on Mouse Tumors

Dimensional Changes

Macroscopic changes in tumor size were evaluated by measuring their diameters using Vernier calipers at the beginning and end of treatment.

Imaging

The changes in tumor size and contrast enhancement were evaluated by means of magnetic resonance imaging (MRI) before and after treatment using 1.5T systems (Avanto; Siemens) and similar pulse sequences. In all cases, coronal short T inversion recovery (STIR), T2-weighted axial turbo spin echo (TSE), and unenhanced T1-weighted axial and coronal TSE sequences were followed by contrast-enhanced, T1-weighted axial and coronal TSE sequences (section thickness 2 mm).

Histology and Biochemical Analyses

After the MRI evaluation, the xenografts were explanted and, depending on tissue availability, the samples were cut into 2 specular halves. One half was fixed in formalin for histological evaluation, and the other was snap frozen for biochemical analysis. The EGFR, AKT, ERK1-2 expression/activation in the lapatinib-treated xenografts was evaluated as described above.

Results

Chordoma Implantation: Outcomes and Growth Characteristics

Stable mouse xenografts were obtained using the tumors of 2 chordoma patients (PDGFRB-positive patient 2 and EGFR-positive patient 5) (Table 1 and Supplementary Fig. 1). The xenografts derived from patient 2 (recurrence, untreated) were lost at the fourth passage, but those derived from patient 5 (primary, untreated) have grown as continuous xenografts for 5 years (2008–2013) and are currently at the ninth passage (P9).

In the case of the 2 chordomas obtained from patients 3 (recurrence, imatinib treated) and 4 (primary, untreated) (Table 1 and Supplementary Fig. 1), the xenografted tumors doubled in size (3 CD-1 *nu/nu* mice per patient), but the animals were lost as a result of intercurrent infection during the third passage after 2 months. It is worth noting that the chordoma tumor derived from patient 3 was removed and engrafted when the patient was progressing on imatinib treatment. As PDGFRB inactivation-mediated drug selection may have favored engraftment, this occurrence was ruled out by means of immunoprecipitation/WB experiments which revealed PDGFRB activation (Supplementary Fig. 1). PDGFRB activation was also confirmed in a local recurrence 2 years later (data not shown).

The engraftments of the samples from patients 1, 6, 7 and 8 (Table 1 and Supplementary Fig. 1) were all unsuccessful (3 CD-1 *nu/nu* mice per patient). In all 4 cases, the tumor specimens were implanted subcutaneously and monitored weekly for a period of 12 months but were gradually reabsorbed.

Visible masses appeared in the mice with the 4 successfully implanted tumors after 3–5 months (Fig. 1A). They generally grew very slowly and reached a size suitable for transplantation in 30–40 weeks, a latency that did not decrease after the first serial passage. In one case (patient 5), the xenografts obtained in the third (20–35 weeks) and fourth passage (10–20 weeks) grew more rapidly and reached a larger volume than all of the other xenografts (Fig. 1B), but this faster growth was no longer observed in the subsequent passages (from the fourth to the ninth, which is still ongoing), and was not accompanied by any morphological or functional changes in comparison with the tumors obtained from the mouse cohort before and after the third and fourth passages.

Successfully Engrafted Human Samples: RTK Profiles and Gene Status

As shown in Fig. 2, all of the human tumor samples had a typical morphology and brachyury nuclear immunostaining and, in line with our previous findings,[4,5] were immunoreactive for PDGFRB and EGFR, and null for HER2/neu. PDGFRB was activated in 6 of the 8 cases, EGFR in 8 of 8, and HER2/neu in 4 of 8 (Supplementary Fig. 1). Occasional large cells with polylobated nuclei were observed in all of the samples and were predominant in patients 2 and 4 (indicated by arrows in Fig. 2).

FISH analyses of the non-polylobated tumoral cell nuclei revealed a normal disomic pattern in all of the probe sets except p16, which was homozygously deleted in patients 2 and 4, and hemizygously deleted in patients 5 and 6 (Supplementary Table 1).

The polylobated nuclei had an abnormal FISH pattern characterized by a very high level of polysomy in all of the tested probe sets (i.e., high-level gains of the evaluated genes and their control probes; see Supplementary Fig. 2). This particular FISH pattern with "amplification" of all of the probes (including the centromere) probably reflected a high level of polyploidy rather than chromosome-specific polysomy. In line with this, the atypical large nuclei in the p16 homozygously deleted cases showed high gains in centromere 9, and the absence of a p16 signal suggested that p16 deletion occurred earlier than polyploidisation.

Interestingly, the FISH signals in some of these large nuclei (both genes and centromeres) appeared to cluster, which suggests genome endoreduplication (i.e., the occurrence of multiple cycles of DNA duplication not followed by mitosis)[18].

Comparison of Human and Xenograft Tumoral Findings

The morphology of all of the successfully engrafted tumors was comparable with that observed in the human samples, and WB revealed brachyury expression (Fig. 3A). The variability in brachyury expression observed by WB (Fig. 3A) could be attributed to the variability in the ratio of tumoral and stromal cells in each sample.

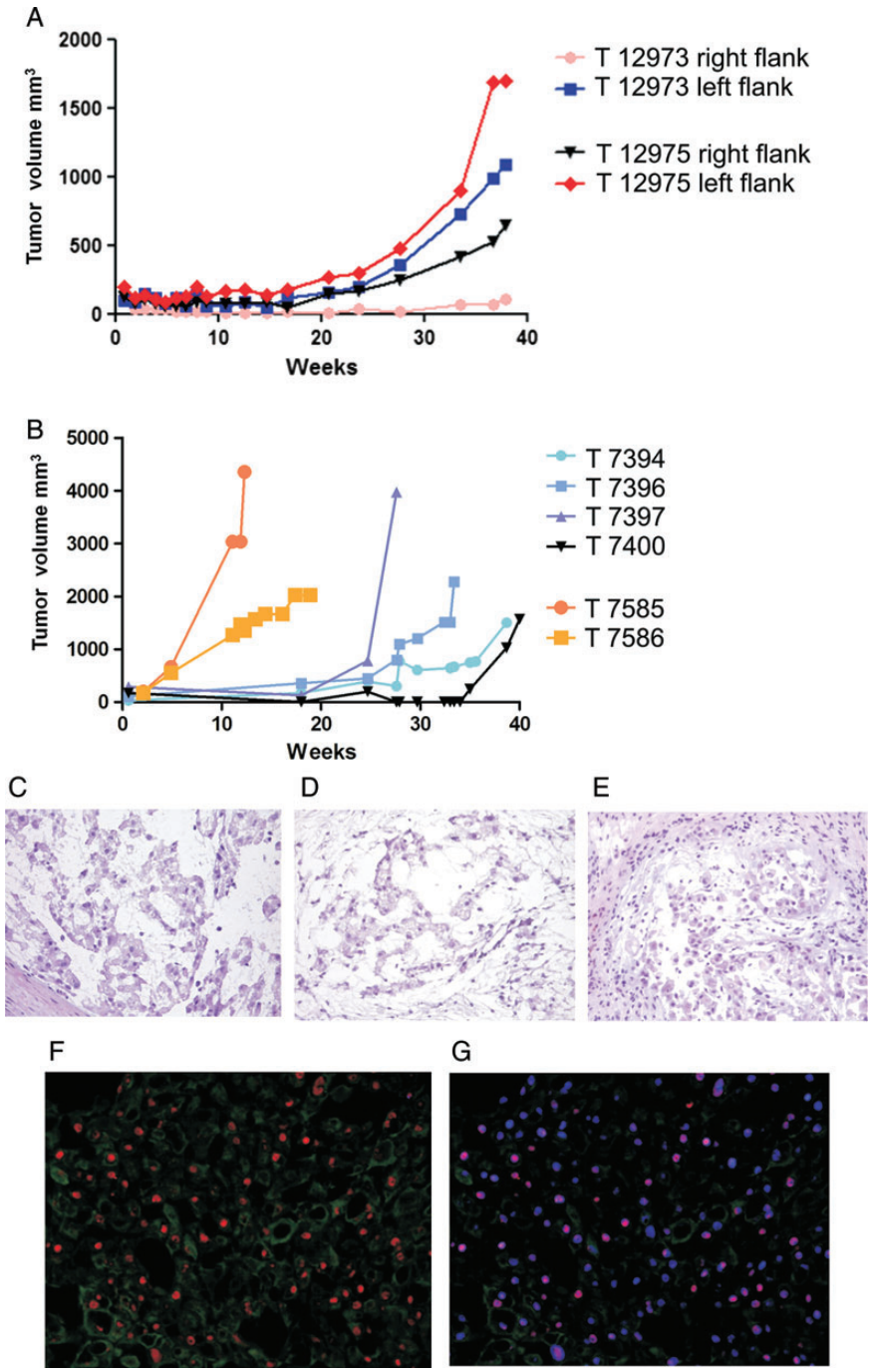

Fig. 1. Growth curves of the chordoma xenograft derived from patient 5. (A) Four fragments were injected into the right and left flanks of 2 CD-1 *nu/nu* mice (T12973 and T12975). Three of the 4 fragments became visible after ~25 weeks (5 months) and were explanted after 40 weeks (8 months). (B) Faster growth and larger volumes were observed during the third (25–40 weeks, T7394, T7396, T7397 and T7400) and fourth passages (10–20 weeks, T7585 and T7586). Morphology (H&E staining) of the human sample implanted in mouse (C) and the xenografts at passage 1 (D) and 4 (E). (F) Brachyury (red signal) and CAM5.2 (green signal) in the T12973 chordoma xenograft. (G) Counterstaining with DAPI (blue signal) showing the brachyury nuclear localization (purple signal). Photomicrographs original magnifications; C, D and E: 100x; F and G: 10X.

Remarkably, the specimens from patients 2 and 4 (which had cells with large polylobated nuclei) retained the same morphological and genetic makeup at each of the transplantation steps (Supplementary Fig. 2).

Signal Transduction Analysis

Since our previous findings in surgically resected human chordoma samples showed that both the PI3K/AKT and RAS/MAPK cascades

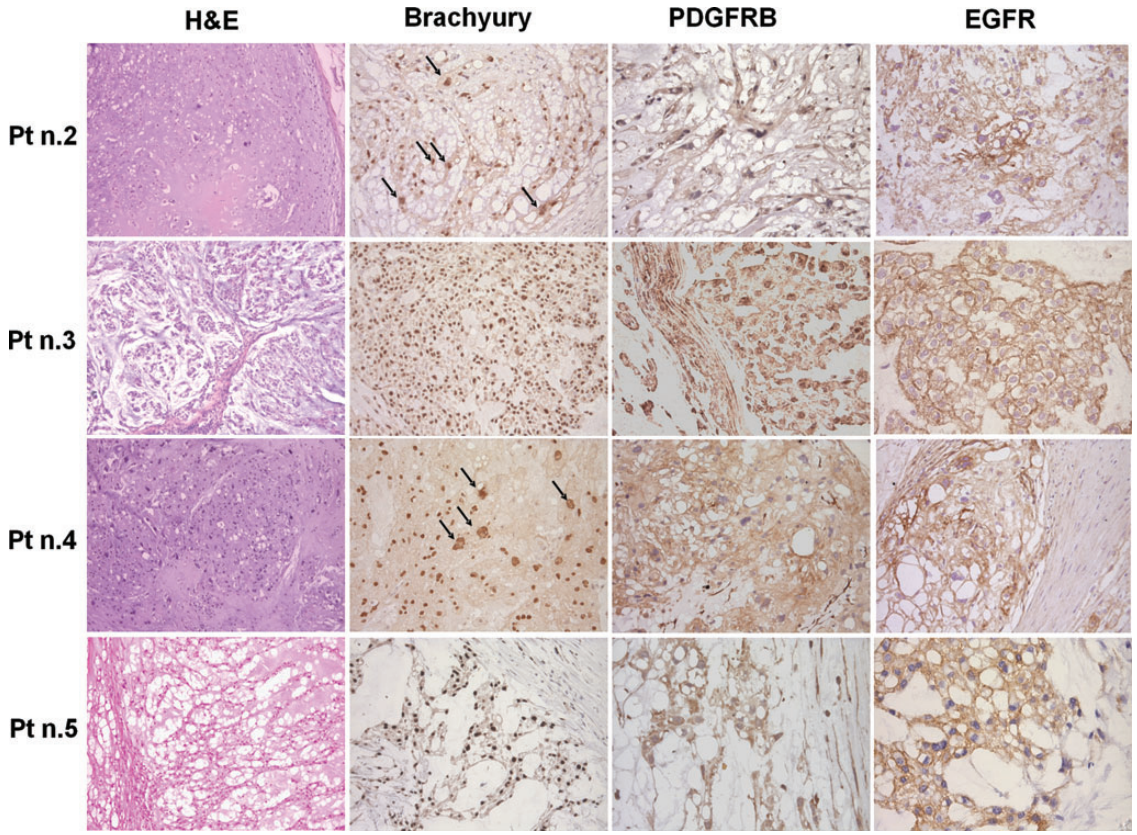

Fig. 2. Morphology (H&E staining), brachyury and RTK immunohistochemistry findings in the 4 successfully implanted chordomas. All of the cases showed physaliferous cells with brachyury nuclear immunostaining as well as cytoplasmatic PDGFRB and mainly membranous EGFR immunostaining. Patients 2 and 4 showed pleomorphic cells with large polylobated nuclei (indicated by the arrows). Photomicrographs original magnifications; H&E staining and brachyury immunohistochemistry: 50x; PDGFRB and EGFR immunohistochemistry: 100x with the exception of EGFR immunostaining of pt n.5 that is 50X.

were activated and that, downstream of mTOR, translational control was preferentially driven by the 4E-BP1/eIF4E pathway.[5] We also compared downstream signaling in the mouse xenografts and corresponding human tumors.

AKT was expressed at all of the transplantation passages, although the level of activation was less than in the corresponding human samples (Fig. 3B). The MAPK cascade was highly expressed and phosphorylated in the human tumors and all of the mouse xenografts. Downstream of mTOR, translational control was dictated by 4E-BP1 protein because, although the S6 protein was expressed, it was activated only in a minority of samples (Fig. 3C).

Overall, the mouse chordomas closely mirrored those observed in the surgical specimens in terms of morphology and interphase cytogenetic characteristics, RTK expression/activation profiles, and downstream signaling.

Characterization and Treatment of Established Xenograft 5

Despite the slow growth, a homogeneous cohort of 7 CD-1 *nu/nu* mice was obtained from the tumor sample of patient 5 at the third passage, when our institute was conducting a prospective phase II study of lapatinib teatment in EGFR/HER2/neu-positive chordoma patients[9]. For this reason, we decided to treat the animals with lapatinib. We first verified the consistency of the human and xenograft RTK activation profiles; both showed evidence of strong EGFR activation as seen in Fig. 4, whereas HER2/neu seemed to be less activated in the xenograft sample. This difference may have been due to the smaller amount of protein that could be extracted from the xenograft, although the possibility that there was actually a difference between the mouse and human tumors cannot be ruled out. We then treated a cohort of 3 mice with lapatinib and used one untreated mouse as a control.

Lapatinib Treatment and its Evaluation

Three third-passage mice were treated by gavage for 21 days with lapatinib 200 mg/kg body weight (the maximum tolerated dose in mouse; G. Manenti Experimental Department, Fondazione IRCCS, Istituto Nazionale Tumori, Milan, Italy, personal communication).

Dimensional Changes and MRI Analysis There was no significant change in the caliper-measured size of any of the treated tumors.

All of the animals underwent MRI at the beginning and end of treatment. The basic MRI pattern of the xenografts was similar to that observed in human patients and was characterized by the presence of mixed and hyperintense lesions. The same was true after the administration of contrast medium, with the lesions showing heterogeneous contrast enhancement.

The untreated mouse (T7395; Fig. 5, panel A) showed no change in tumor size but an increase in contrast enhancement (+20.0%,

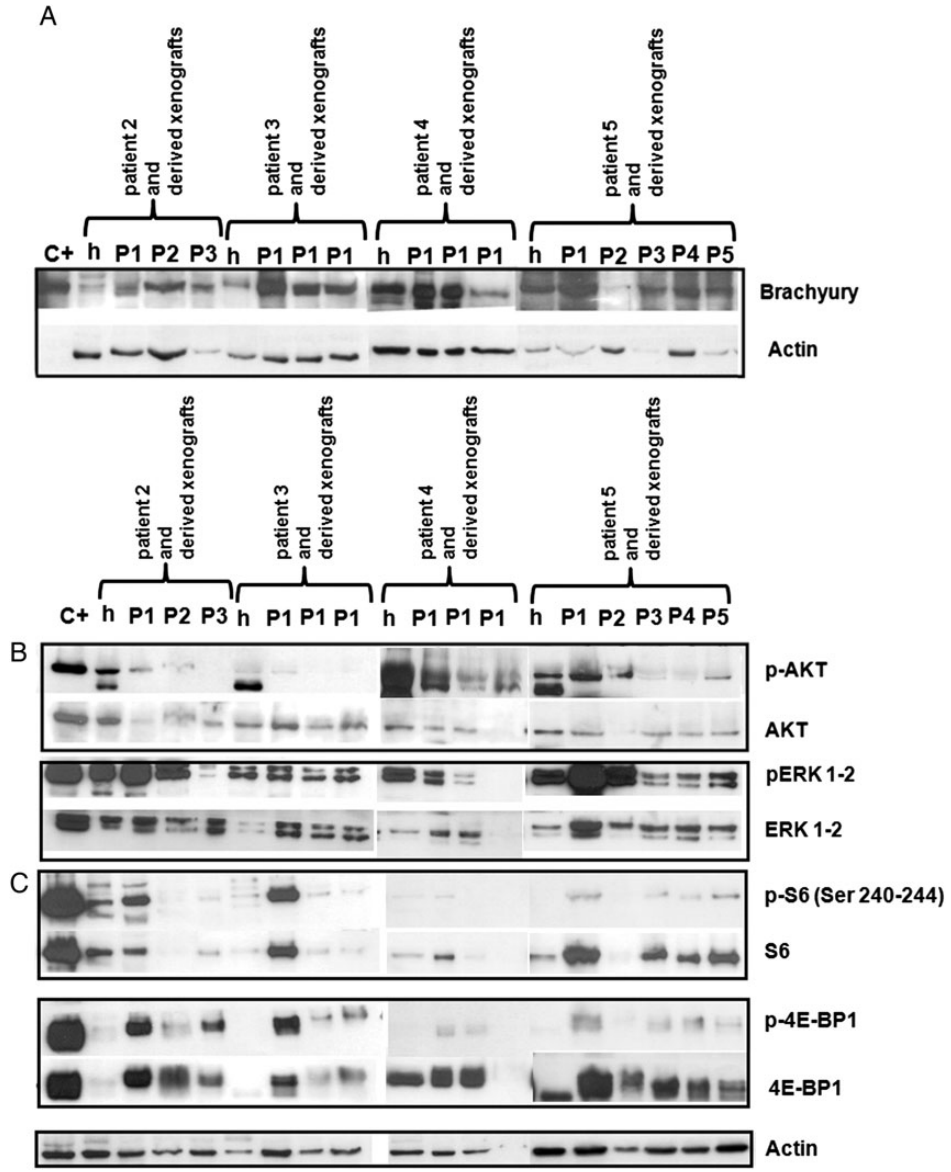

Fig. 3. WB-based brachyury and signal transduction. (A) Like the corresponding human tumor samples (h), the xenografts derived from patients 2, 3, 4 and 5 expressed brachyury throughout all of the transplantation steps (P). (B and C) In the xenograft samples, the MAP cascade (ERK1-2) and 4E-BP1 were more activated than AKT or S6. C+: positive controls.

Supplementary Table 2). Treated mice T7398 and T7400 did not show any change in tumor size, but contrast enhancement decreased in all of the evaluated lesions (Fig. 5, panel A and Supplementary Table 2). A more complex imaging pattern was found in treated mouse T7394, which developed a new pelvic lesion after treatment (circled in Fig. 5, panel A), whereas the thoracic lesion showed decreased contrast enhancement (Fig. 5, panel A and Supplementary Table 2). Taken together, these results suggest that MRI is more suitable than calipers for evaluating tyrosine kinase inhibitor (TKI) responses in chordoma xenografts, as previously observed in chordoma patients undergoing TKI treatment.[7]

Pathological and Biochemical Responses Histologically, the treated lesions had a few small areas with an appreciable reduction in cellularity (Fig. 5, panel B), but these did not correlate with the MRI finding of decreased contrast enhancement. WB for cleaved caspase 3 was consistently negative in the lapatinib-treated xenografts (Supplementary Fig. 3).

Biochemical analysis showed EGFR and signaling activation in the dimensionally progressing lesions of mouse T7394 that was comparable with that observed in the untreated mouse, and there was significant switching off of EGFR, AKT and ERK1-2 in the lesions of mice T7398 and T7400 characterized by decreased contrast enhancement (Fig. 5, panel C).

Discussion

This paper describes the establishment, characterization and treatment of chordoma xenografts obtained from the

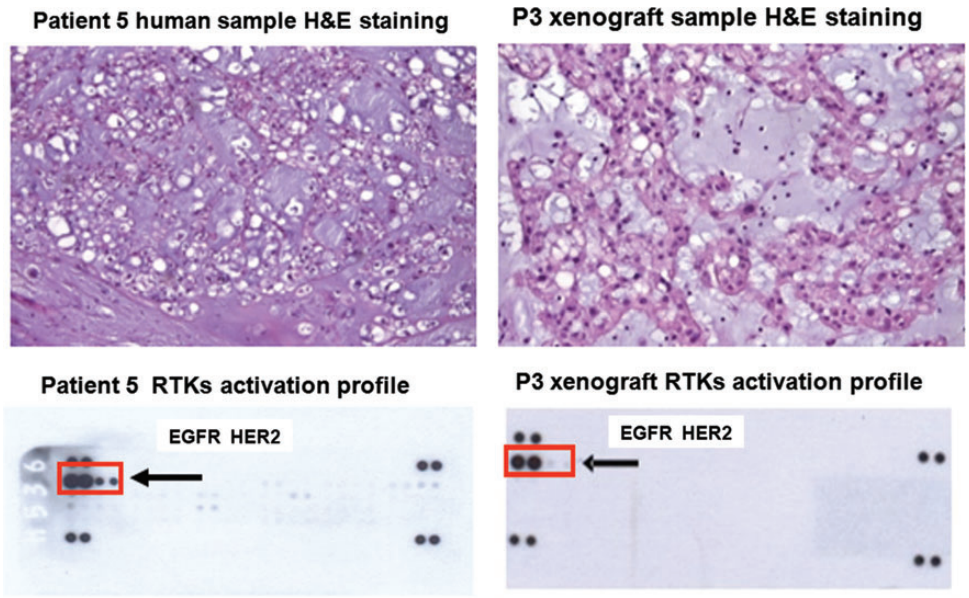

Fig. 4. Comparison of the morphology (H&E staining) and RTK activation profile (pRTK assay) of the frozen samples obtained from patient 5 and the corresponding third passage xenograft. Their morphology was similar, and both showed evidence of strong EGFR activation, whereas HER2/neu seemed to be weakly activated in the xenograft (box and arrows). Photomicrographs original magnifications; patient 5 human sample:100x, P3 xenograft sample: 200X.

subcutaneous injection of human surgical specimens, and the data confirm recently published findings[10] that tumors developed in mice retain most of the features of the original human tumors. Moreover, pharmacological treatment provided the first "proof of principle" that chordoma mouse xenografts can be used as a preclinical model for targeted therapies. This is particularly relevant because chordomas are only moderately sensitive or even insensitive to standard chemotherapy,[2] and targeted therapies[3–6] are now becoming a viable option, but the lack of preclinical models that recapitulate the organization and functions of human chordoma is a critical factor hindering improvements in medical treatment. Cell lines only partially reflect the original tumor microenvironment because they lack a vascular supply, extracellular matrix, and paracrine signals, all of which may play a role in tumor growth and resistance to targeted treatments.[15] Furthermore, mouse engraftments should avoid the selective pressure due to in vitro propagation that probably explains the divergence of cell lines from real human tumors.[19]

We were able to maintain tumor growth for more than 4 years in our CD-1 *nu/nu* mice, which are less immunocompromised and easier to handle than the NOD/SCID/interleukin 2 receptor $[IL2r]^{null}_{\gamma}$ mouse used to obtain the xenograft of the human U-CH1 cell line.[12] The main drawback of our model is the long and extremely variable time needed for tumor growth, which means that it takes a long time to obtain the tumor masses needed for pharmacological experiments. More importantly, the number of animals obtained at each passage is always low; this prevents experimental planning, which requires large animal cohorts. Whether this slow growth mirrors the indolent behavior of the human disease[1] or represents a restraint due to subcutaneous implantation will need to be verified using an orthotopic (bone) model. Unfortunately, bone implantations cause animal pain and stress, which conflicts with the European guidelines concerning animal experiments. We chose to use subcutaneous implantations because chordoma metastases are frequently subcutaneous, and we reasoned that a subcutaneous microenvironment can permit chordoma growth as much as bone. Furthermore, it is easy to monitor the growth of a subcutaneous tumor.

Another possible limitation of our xenograft model could be the selection of more aggressive tumors, as in the case of breast cancer[19] and myxoid liposarcoma xenografts.[20] In line with this, the chordoma sample from patient 5 showed greater EGFR-HER2/neu activation than any of the other patient samples (Supplementary Fig. 1).

During the period of the present study, our institute was conducting a now-completed phase II study of lapatinib involving EGFR-HER2/neu-positive patients with advanced chordoma,[9] and xenograft 5 came from one of these patients. Although not representative of the more frequently encountered PDGFRB-positive chordomas treated with imatinib,[3,4] this xenograft allowed us to shed light on possible histological changes (pathological responses) that could not be considered in the study patients because the protocol did not include a posttreatment biopsy. In addition, the pre- and posttreatment comparisons of the xenograft treated with lapatinib made it possible to correlate the MRI imaging, immunohistochemistry, and biochemistry findings. The lapatinib-induced incomplete and heterogeneous switching off of EGFR and its signaling in our model, which was not sustained by resistant mutations (data not shown), suggesting slight drug activity in human patients. Interestingly, the degree of EGFR inactivation, which seems to parallel the decrease in imaging contrast enhancement, closely suggests that MRI could be used for the early evaluation of the efficacy of targeted therapies. In line with this, and confirming the usefulness of our xenograft model, slight

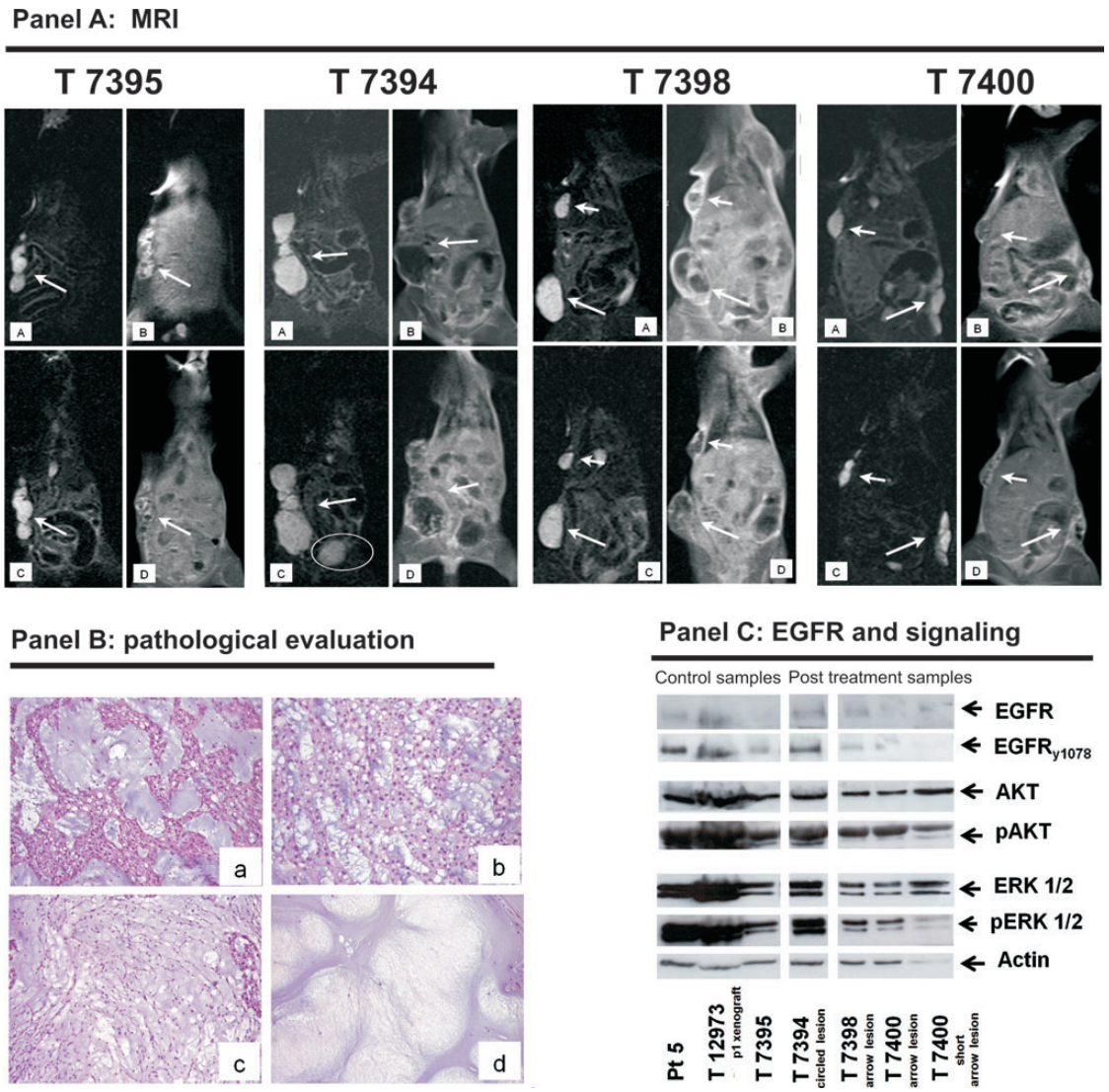

Fig. 5. Evaluation of lapatinib treatment results in xenograft 5. Panel A. MRI coronal STIR images without (A and B) and with contrast medium (C and D). Mouse 7395 was used as an untreated control. A and B) One hyperintense subcutaneous lesion at baseline (arrow). C and D) After 3 weeks off treatment, there was no substantial variation in tumor size, but there was an increase in tumor contrast enhancement (+20%, Supplementary Table 2). Before lapatinib treatment, the treated mice 7398 and 7400 (A and B) showed hyperintense subcutaneous lesions (arrows and short arrows). After treatment (C and D), there was no substantial variation in size, but all of the lesions showed a decrease in tumor contrast enhancement (see Supplementary Table 2 for details). Before lapatinib treatment, treated mouse 7394 (A and B) showed one hyperintense lateral thoracic subcutaneous lesion (arrow). After treatment, the thoracic lesion showed a decrease in tumor contrast enhancement (C and D) but a new small caudal lesion (circled) appeared (see Supplementary Table 2 for details). Panel B. Morphological evaluation. In comparison with untreated mouse 7395 (a), and regardless of MRI responses, all of the treated mice showed nonresponsive areas (b) and few decellulated (i.e., responsive) areas (c and d). Panel C. Biochemical results. In line with the MRI responses, the switching off of EGFR, AKT and ERK1-2 was more pronounced in mice 7398 and 7400 than in mouse 7395 (untreated) or mouse 7394 (circled lesion). The EGFR activation observed in frozen samples obtained from patient 5 (pt5) and the first passage xenograft (T12973) was used as positive control. Photomicrographs original magnifications: 50X.

clinical activity was found in the chordoma participants in the prospective phase II study of lapatinib.[9]

In conclusion, our results suggest that chordomas recapitulating the characteristics of human chordomas can grow in nude mice and that newly established chordoma xenografts are a powerful means of investigating the biology of chordomas and developing more selective and effective tailored treatments, including the recently proposed and more sophisticated brachyury-based gene therapy[12,21].

Supplementary material

The supplementary material is available on line at *Neuro-Oncology* (http://neuro-oncology.oxfordjournals.org).

Funding

Supported by a Chordoma Foundation grant to ET, and an AIRC grant (R/10/029) to SP. EC fellowship was supported by Famiglia Visioli.

Conflict of interest statement. None declared.

References

1. Stacchiotti S, Casali PG, Lo Vullo, et al. Chordoma of the mobile spine and sacrum: a retrospective analysis of a series of patients surgically treated at two referral centers. *Ann Surg Oncol*. 2010;17(1):211–219.
2. Chugh R, Dunn R, Zalupski MM, et al. Phase II study of 9-nitro-camptothecin in patients with advanced chordoma or soft tissue sarcoma. *J Clin Oncol*. 2005;23(15):3597–3604.
3. Casali PG, Messina A, Stacchiotti S, et al. Imatinib mesylate in chordoma. *Cancer*. 2004;101(9):2086–2097.
4. Tamborini E, Miselli F, Negri T, et al. Molecular and biochemical analyses of platelet-derived growth factor receptor (PDGFR) B, PDGFRA, and KIT receptors in chordomas. *Clin Cancer Res*. 2006;12(23):6920–6928.
5. Tamborini E, Virdis E, Negri T, et al. Analysis of receptor tyrosine kinases (RTKs) and downstream pathways in chordomas. *Neuro Oncol*. 2010; 12(8):776–789.
6. Shalaby A, Presneau N, Ye H, et al. The role of epidermal growth factor receptor in chordoma pathogenesis: a potential therapeutic target. *J Pathol*. 2011;223(3):336–346.
7. Stacchiotti S, Longhi A, Ferraresi V, et al. Phase II study of imatinib in advanced chordoma. *J Clin Oncol*. 2012;30(9):914–920.
8. Stacchiotti S, Marrari A, Tamborini E, et al. Response to imatinib plus sirolimus in advanced chordoma. *Ann Oncol*. 2009;20(11): 1886–1894.
9. Stacchiotti S, Tamborini E, Lo Vullo S, et al. Phase II study on lapatinib in advanced EGFR-positive chordoma. *Ann Oncol*. 2013;24(7): 1931–1936.
10. Siu IM, Salmasi V, Orr BA, et al. Establishment and characterization of a primary human chordoma xenograft model. *J Neurosurg*. 2012;116(4): 801–809.
11. Park DM. Chordoma model. *J Neurosurg*. 2012;116(4):799–800.
12. Presneau N, Shalaby A, Ye H, et al. Role of the transcription factor T (brachyury) in the pathogenesis of sporadic chordoma: a genetic and functional-based study. *J Pathol*. 2011;223(3):327–335.
13. Nelson AC, Pillay N, Henderson S, et al. An integrated functional genomics approach identifies the regulatory network directed by brachyury (T) in chordoma. *J Pathol*. 2012;228(3):274–285.
14. Schwab JH, Boland PJ, Agaram NP, et al. Chordoma and chondrosarcoma gene profile: implications for immunotherapy. *Cancer Immunol Immunother*. 2009;58(3):339–349.
15. Muranen T, Selfors LM, Worster DT, et al. Inhibition of PI3 K/mTOR leads to adaptive resistance in matrix-attached cancer cells. *Cancer Cell*. 2012;21(2):227–239.
16. Mirra JM, Della Rocca C, Nelson and Mertens F. *World Health Organization Classification of Tumours. Pathology and Genetics, Tumours of Soft Tissue and Bone*. IARC Press: Lyon, 2002; 315–316.
17. Amin DN, Sergina N, Ahuja D, et al. Resiliency and vulnerability in the HER2-HER3 tumorigenic driver. *Sci Transl Med*. 2010;2(16).16ra7: 1–9.
18. Grafi G. Cell cycle regulation of DNA replication: the endoreduplication perspective. *Exp Cell Res*. 1998;244(2):372–378.
19. DeRose YS, Wang G, Lin YC, et al. Tumor grafts derived from women with breast cancer authentically reflect tumor pathology, growth, metastasis and disease outcomes. *Nat Med*. 2011;17(11): 1514–1520.
20. Frapolli R, Tamborini E, Virdis E, et al. Novel models of myxoid liposarcoma xenografts mimicking the biological and pharma-cologic features of human tumors. *Clin Cancer Res*. 2010;16(20): 4958–4967.
21. Pillay N, Plagnol V, Tarpey PS, et al. A common single-nucleotide variant in T is strongly associated with chordoma. *Nat Genet*. 2012;44(11): 1185–1187.